


State-dependent mean-field formalism to model different activity states in conductance-based networks of spiking neurons

Cristiano Capone ^{*}*INFN, Sezione di Roma, 00185 Rome, Italy**and Department of Integrative and Computational Neuroscience (ICN), Paris-Saclay Institute of Neuroscience (NeuroPSI),
Centre National de la Recherche Scientifique (CNRS), 91198 Gif-sur-Yvette, France*

Matteo di Volo

*Department of Integrative and Computational Neuroscience (ICN), Paris-Saclay Institute of Neuroscience (NeuroPSI),
Centre National de la Recherche Scientifique (CNRS), Laboratoire de Physique Théorique et Modélisation,
Université de Cergy-Pontoise, 95302 Cergy-Pontoise cedex, France*

Alberto Romagnoni

*Data Team, Département d'informatique de l'ENS, École normale supérieure France, CNRS, PSL Research University, 75005 Paris France
and Centre de recherche sur l'inflammation UMR 1149, Inserm-Université Paris Diderot, Paris, France*Maurizio Mattia *National Center for Radiation Protection and Computational Physics, Istituto Superiore di Sanità, 00161 Rome, Italy*Alain Destexhe *Department of Integrative and Computational Neuroscience (ICN), Paris-Saclay Institute of Neuroscience (NeuroPSI),
Centre National de la Recherche Scientifique (CNRS), 91198 Gif-sur-Yvette, France*

(Received 7 March 2019; revised manuscript received 12 October 2019; published 23 December 2019)

More interest has been shown in recent years to large-scale spiking simulations of cerebral neuronal networks, coming both from the presence of high-performance computers and increasing details in experimental observations. In this context it is important to understand how population dynamics are generated by the designed parameters of the networks, which is the question addressed by mean-field theories. Despite analytic solutions for the mean-field dynamics already being proposed for current-based neurons (CUBA), a complete analytic description has not been achieved yet for more realistic neural properties, such as conductance-based (COBA) network of adaptive exponential neurons (AdEx). Here, we propose a principled approach to map a COBA on a CUBA. Such an approach provides a state-dependent approximation capable of reliably predicting the firing-rate properties of an AdEx neuron with noninstantaneous COBA integration. We also applied our theory to population dynamics, predicting the dynamical properties of the network in very different regimes, such as asynchronous irregular and synchronous irregular (slow oscillations). This result shows that a state-dependent approximation can be successfully introduced to take into account the subtle effects of COBA integration and to deal with a theory capable of correctly predicting the activity in regimes of alternating states like slow oscillations.

DOI: [10.1103/PhysRevE.100.062413](https://doi.org/10.1103/PhysRevE.100.062413)

I. INTRODUCTION

Recent developments in recording techniques are shedding light on the dynamics of cortical neural networks in higher and higher spatiotemporal detail [1]. There are different scientific ways to investigate and understand such large amounts of data. A first class of approaches are top-down, aiming to use data as a constrain to build generative models capable to automatically reproduce statistical features observed in experiments [2–5]. However, it is possible to interpret the experimental observed behavior by mean of a bottom-up theoretical model. To achieve this, different levels of description

are possible, ranging from single spiking neurons [6,7] to population model [8–15], from extremely detailed [8,16–18] to more coarse-grained models [19,20].

While keeping the model as simple as possible, it has been recently shown that some minimal requirements are necessary to reproduce a rich repertoire of dynamical features. In particular, a quite refined model as the AdEx is necessary to describe a response on a broad range of frequencies [21]. Moreover, voltage-dependent synapses have been largely shown to be a crucial mechanism of neurons' interaction [22,23]. While direct simulation of large ensembles of single neurons can be performed, such an approach can be computationally heavy and does not permit a straightforward understanding of the system dynamics. A principled dimensional reduction approach such as mean-field (MF) theories are powerful and

^{*}cristiano.capone@roma1.infn.it

TABLE I. Neuronal parameters defining the two populations RS-FS model.

	θ (mV)	τ_m (ms)	C (nF)	E_l (mV)	ΔV (mV)	τ_i (ms)	E_i (mV)	Q_i (nS)	b (nA)	τ_w (s)
RS	-50	20	0.2	-65	2.0	5	0	1	0.005	0.5
FS	-50	20	0.2	-65	0.5	5	-80	5	0	0.5

widespread tools, used to obtain a large-scale description of neuronal populations. One of the first successful attempts was to provide a theory to describe leaky integrate and fire neurons with current-based input [14,19,24,25], where the firing-rate properties of the neurons are described as a function of the statistics of its input current through a Fokker-Planck formalism. This approach was also successfully exploited to work out asymptotic firing rates under mean-field approximation incorporating synaptic filters [26,27]. For relatively small synaptic timescales this leads to an effective current-to-rate gain function equivalent to the one for instantaneous synaptic transmission with a perturbative modulation of the firing threshold.

The description of the asymptotic firing rates when conductance-based inputs under mean-field approximation has also a long track of successful attempts [15,28–30]. However, neither current fluctuations nor synaptic filters was taken into account simultaneously. In the same framework, the dynamics beyond the asynchronous linearizable state has been addressed by numerically integrating the Fokker-Planck equation [31–33], while theoretical insights have been obtained only for specific quasi-stationary conditions [15,33].

However, taking into account these modeling features all together in an excitatory-inhibitory network is extremely challenging. Only recently, a method was proposed based on a semianalytic approach [34,35] that can give satisfactory quantitative predictions also for networks with adaptation and slow wave activity [36]. Nevertheless, this method is based on a fitting procedure for the transfer function in regimes with relatively low activity and low synchronization. Accordingly, it is still far from a full analytic approach that would capture different dynamical brain states. Steps in this direction are not only a mere exercise of elegance but permit a deeper understanding of the role played by model features (e.g., voltage-dependent interactions) for the emerging dynamics. As we will describe in this manuscript, thanks to such an approach we found out that neurons work in two main regimes as different approximations can lead to two different analytic results. In particular, each of the two approximations only work in a specific dynamical condition, that can be either drift- or fluctuation-driven. Moreover, in light of these results, we propose here a principled state-dependent approximation, where we use two approximations valid in the two limits described above, and which can be analytically merged. This allows us to define a current-to-rate gain function reliable also in regimes where the dynamics is not strictly drift or fluctuation driven.

One of the main functions introduced here is an effective current-to-rate gain function aimed at simplifying the theoretical description of the dynamics of networks composed of COBA neurons. This allowed us to make a step further in terms of usability of the theory also for numerical integration of the mean-field dynamics, compared to the double-integral expression provided in Refs. [28,30].

Our approach turns out to be rather effective for investigating the properties of neuronal populations dynamics. In particular, we considered a network composed of excitatory and inhibitory neurons, namely, the standard minimal circuitry for cortical neuronal networks [37,38]. The network parameters are set to reproduce two different dynamical conditions that are biologically relevant, i.e., asynchronous irregular and slow oscillating dynamics [39]. We show that both of them are reliably described by our mean-field model and that the state-dependent approach is indispensable to achieve the quality of such result.

Furthermore, our approach is particularly convenient to compare dynamical properties of CUBA and COBA networks. In particular, we investigated the effect of the network integration of multiple incoming inputs. We found, in accordance with Ref. [23], that COBA networks have a stronger sublinear suppression, which is important to account for experimental observations. This is also an interesting feature in terms of computational capabilities, since the presence of COBA synapses plays an important role for networks to disambiguate stimuli.

II. RESULTS

A. Neuronal network model

We derive a state-dependent current-to-rate gain function for conductance-based (COBA) AdEx-type neurons, whose dynamics evolves according to the following equations [7]:

$$\begin{aligned} \frac{dV(t)}{dt} &= -\frac{V(t)-E_l}{\tau_m} + \frac{\Delta V}{\tau_m} e^{[\frac{V(t)-\theta}{\Delta V}]} + \frac{I[t,V(t)]}{C} - \frac{W(t)}{C} \\ \frac{dW(t)}{dt} &= -\frac{W(t)}{\tau_w} + b \sum_k \delta(t-t_k) + a[V(t) - E_l] \end{aligned} \quad (1)$$

where the synaptic input I is defined as

$$I[t, V(t)] = \sum_{\alpha} g_{\alpha}(t)[V(t) - E_{\alpha}], \quad (2)$$

and where $V(t)$ is the membrane potential of the neuron and $\alpha = e, i$ defines the excitatory (e) and the inhibitory (i) input. The parameters of the neurons, which depend on the populations they belong to (excitatory RS or inhibitory FS, see Table I), are τ_m the membrane time constant, C the membrane capacitance, E_l the reversal potential, θ the threshold, ΔV the exponential slope parameter, W the adaptation variable, and a and b are the adaptation parameters. g_{α} are the synaptic conductances, defined as

$$g_{\alpha}(t) = \sum_k \Theta(t-t_k) Q_{\alpha} \exp[-(t-t_k)/\tau_{\alpha}]. \quad (3)$$

We define the spiking time of the neuron when the membrane potential reaches the threshold $V_{\text{spike}} = \theta + 5\Delta V$. t_k^{α} indicates the times of presynaptic spikes received by the

neuron from synapse type α with characteristic time τ_α and its synaptic efficacy Q_α .

B. Current-to-rate gain function

Under the assumption of quasi-instantaneous synaptic transmission (negligible τ_α), for a neuron described by the dynamical system of Eq. (1) it is possible to write a Fokker-Planck equation describing the dynamics of the probability density function (p.d.f.) for its membrane potential V as

$$\tau_m \frac{\partial p(V, t)}{\partial t} = \frac{\partial}{\partial V} [(f(V) + \mu)p(V, t)] + \frac{\sigma^2}{2} \frac{\partial^2}{\partial V^2} p(V, t), \quad (4)$$

where $f(V) = -(V(t) - E_l) + \Delta V e^{\frac{V(t)-\theta}{\Delta V}}$ and suited boundary conditions are taken into account [40], i.e., an absorbing barrier at the spike emission threshold $V_{\text{spike}} = \theta + k\Delta V$ (k is arbitrarily chosen to be 5, its value weakly affects the spike timing) and that the probability current $[f(V) + \mu]p(V, t) + \frac{1}{2}\sigma^2 \partial_V p(V, t)|_{V=V_{\text{spike}}}$ is reinjected in $V_{\text{reset}} = -65$ after a refractory period $\tau_{\text{arp}} = 5$ ms. We assumed that the input $\frac{I(t)}{C}$ is a white noise with infinitesimal mean μ and infinitesimal variance σ [Fig. 1(a)]. This means that the first line of Eq. (1) would be rewritten as

$$dV(t) = \left[-\frac{V(t) - E_l}{\tau_m} + \frac{\Delta V}{\tau_m} e^{\frac{V(t)-\theta}{\Delta V}} - \frac{W(t)}{C} \right] dt, \quad (5)$$

$$+ \mu dt + \sigma \xi(t) \sqrt{dt},$$

where $\xi(t)$ is a Gaussian white noise. Under stationary conditions, the firing rate of the neuron is given by the flux of realizations (i.e., the probability current) crossing the threshold V_{spike} [24]:

$$\mathcal{F}(\mu, \sigma) = \frac{1}{\sigma^2} \int_{-\infty}^{\theta+5\Delta V} dV \int_{\max(V, V_r)}^{\theta+5\Delta V} du \quad (6)$$

$$\times e^{-\frac{1}{\tau_m \sigma^2} \int_V^u [f(v) + \mu \tau_m] dv}.$$

Such a function, usually referred to as a transfer function (or current-to-rate gain function), provides an estimate of neuronal firing rate which is in remarkable agreement with the one measured from numerical integration of Eq. (1) [Fig. 1(b)]. Nevertheless, in the case of voltage-dependent synapses determining the infinitesimal moments of the input current (mean μ and variance σ^2) as a function of the input firing rate is not straightforward.

In particular when a conductance-based input is considered [Fig. 1(c)], the stochastic process describing the input current has voltage-dependent infinitesimal mean and variance due to the voltage-dependent nature of the impact of the incoming spikes on the membrane potential dynamics [Fig. 1(d)]. In this framework, an explicit solution of the aforementioned Fokker-Planck equation has not yet been worked out.

1. Moment closure (MC) approximation

One of the major problems in modeling COBA neurons is that the input current is voltage-dependent and can be

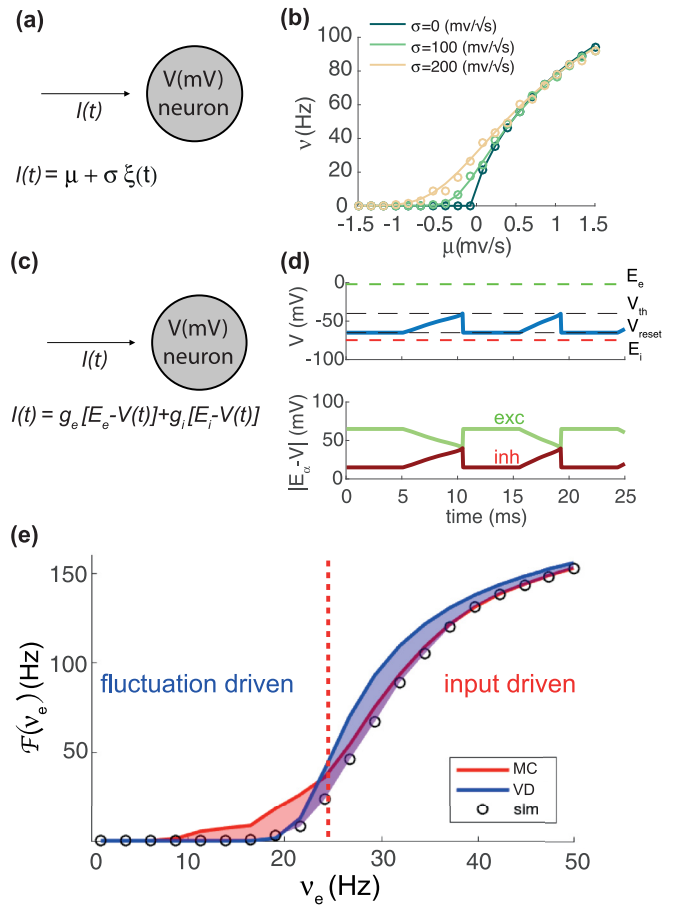


FIG. 1. Current-to-rate gain function for AdEx neurons with conductance-based input: (a) Sketch of an AdEx neuron with current-based input represented by a white noise. (b) Current-to-rate gain function $\mathcal{F}(\mu, \sigma)$ for AdEx neuron receiving a white noise input with mean and variance (μ and σ , respectively). Theory and simulations (lines and circles, respectively) are in remarkable agreement. (c) Sketch of an AdEx neuron with conductance-based (COBA) input. (d) Graphic presentation of the voltage dependence of the conductance-based input. (e) Firing rate of neuron with COBA input as a function of the excitatory input and with constant inhibitory one (circles). Two different theoretical approximations in red (light gray) and blue (dark gray).

written as

$$I(t) = \sum_{\alpha=e,i} [\bar{g}_\alpha (E_\alpha - \bar{V}) - \bar{g}_\alpha \delta V + \delta g_\alpha \bar{V} - \delta g_\alpha \delta V], \quad (7)$$

where we wrote V and g_α as their average value plus their time-dependent variations ($V = \bar{V} + \delta V$ and $g_\alpha = \bar{g}_\alpha + \delta g_\alpha$). A first naive approximation consists in replacing the variable V by its average \bar{V} , such that the input current $I = g_e(E_e - \bar{V}) + g_i(E_i - \bar{V})$ is now independent from V . Under diffusion approximation (i.e., in the limit of small g_i and g_e , and a large rate of incoming spikes), the two infinitesimal moments μ and σ^2 of I are:

$$\mu = \frac{\bar{g}_e(E_e - \bar{V}) + \bar{g}_i(E_i - \bar{V})}{C} \quad (8)$$

$$\sigma^2 = \frac{\sigma_{g_e}^2 (E_e - \bar{V})^2 + \sigma_{g_i}^2 (E_i - \bar{V})^2}{C^2}.$$

Since μ and σ can be written as a function of the firing rate, it is possible to write the transfer function as

$$\mathcal{F}(v_e, v_i) = \frac{1}{\sigma^2} \int_{-\infty}^{\theta+5\Delta V} dV \int_{\max(V, V_r)}^{\theta+5\Delta V} du \times e^{-\frac{1}{\tau_m \sigma^2} \int_V^u [f(v) + f_1(v, \bar{g}_e, \bar{g}_i)] dv}. \quad (9)$$

This equation is the same as Eq. (6) where $\mu = f_1(\bar{v}, \bar{g}_e, \bar{g}_i)/\tau_m$ due to Eq. (8). Comparing this expression with numerical simulations of the single-neuron spiking activity in Fig. 1(e) [red (light gray) line], a good agreement is mainly apparent under drift-driven regime ($\mu \tau_m > \theta$).

2. Voltage-dependent (VD) approximation

It is also possible to take into account the dependence of the input current $I(t)$ on the voltage [28,30,41,42] by writing it in the following way:

$$I(t) = \sum_{\alpha=e,i} [\bar{g}_\alpha(E_\alpha - \bar{V}) - \bar{g}_\alpha \delta V + \delta g_\alpha \bar{V} - \delta g_\alpha \delta V] \simeq \sum_{\alpha=e,i} [\bar{g}_\alpha(E_\alpha - \bar{V}) - \bar{g}_\alpha \delta V + \delta g_\alpha \bar{V}]. \quad (10)$$

In the last step, the term $-\sum_\alpha \delta V \delta g_\alpha$ has been neglected since δV is assumed to be of the same order as δg_α [30,41], so $\delta V \delta g_\alpha \sim O[(\delta g_\alpha)^2]$. Under this approximation, the synaptic current can be then written as a deterministic voltage-dependent part plus a stochastic component which is independent from V . As we are considering a quasi-instantaneous synaptic transmission ($\tau_\alpha \simeq 0$), such stochastic source of current can still be modeled by a Gaussian white noise [24] such that

$$I = f_1(V, \bar{g}_e, \bar{g}_i) + \sigma \xi(t), \quad (11)$$

where $\sigma = \sqrt{\frac{\sigma_{\bar{g}_e}^2 (E_e - \bar{V})^2 + \sigma_{\bar{g}_i}^2 (E_i - \bar{V})^2}{C^2}}$, $\xi(t)$ is a white noise $\mathcal{N}(0, 1)$ and $f_1(V, \bar{g}_e, \bar{g}_i) = \bar{g}_e(E_e - V) + \bar{g}_i(E_i - V)$, with \bar{g}_e, \bar{g}_i and $\sigma_{\bar{g}_e}^2, \sigma_{\bar{g}_i}^2$ the mean and the variance of the synaptic conductances, respectively. In the case of input spike trains with Poissonian statistics these infinitesimal moments result to be [24,43,44]

$$\bar{g}_\alpha = \tau_\alpha Q_\alpha K_\alpha \nu_\alpha \quad (12)$$

$$\sigma_{\bar{g}_\alpha}^2 = \frac{\tau_\alpha Q_\alpha^2 K_\alpha \nu_\alpha}{2},$$

where K_α is the number of synaptic contact each neuron receives from the population $\alpha \in \{e, i\}$.

As above, considering $f_1(V)$ as an additional term to $f(V)$, it is again possible to work out an analytic expression for the transfer function:

$$\mathcal{F}(\bar{g}_e, \bar{g}_i, \sigma) = \frac{1}{\sigma^2} \int_{-\infty}^{V_{up}} dV \int_{\max(V, V_r)}^{V_{up}} du \times e^{-\frac{1}{\tau_m \sigma^2} \int_V^u [f(v) + f_1(v, \bar{g}_e, \bar{g}_i)] dv}. \quad (13)$$

The result of such approximation is shown in Fig. 1(e) [blue (dark gray) line]. We observe that this approximation gives good theoretical prediction as far as the average membrane potential of the neuron is sufficiently low (i.e., under noise-dominated regime).

C. A mixed framework: State-dependent (SD) approximation

The two proposed approximations rely on different assumptions of the composition of the input current $I(t)$ to the neurons, which turned out to be valid under different dynamical regimes of the neuron. In this paragraph we propose a mixed framework to have a continuous transfer function, by introducing a new parameter that allows us to interpolate between the two regimes. This parameter is introduced not by an *a posteriori* fit but by *a priori* considerations on the input current.

Under drift-dominated regime ($\mu \tau_m > \theta$), the spiking times are mainly determined by the deterministic component of the input and not by the stochastic one.

Accordingly, neglecting V fluctuations and replacing it with its average value, is a good assumption and the use of MC approximation is very satisfactory [Fig. 1(e), left side].

When $\mu \tau_m < \theta$, i.e., under *fluctuation-driven* regime, the neuron can only fire in presence of large-enough subthreshold fluctuations, as $\bar{V} \ll \theta$. Therefore, all the variability of V has to be taken into account, as subthreshold suppression appears when V is close to the θ . Under this condition, VD approximation result to be the most effective [Fig. 1(e), right], as the additional term $-\sum_\alpha \bar{g}_\alpha \delta V$ in the current $I(t)$ is taken into account. This term is lacking in the MC approximation.

Starting from that, we unify these two expressions for \mathcal{F} by writing

$$I(t) = \sum_{\alpha=e,i} [\bar{g}_\alpha(E_\alpha - \bar{V}) + \delta g_\alpha \bar{V} - (1-s)\bar{g}_\alpha \delta V], \quad (14)$$

where s is an arbitrary state-dependent parameter which is 0 when $\bar{V} \ll \theta$ and 1 when \bar{V} approaches θ as

$$s = \frac{1}{1 + \exp\left[-\frac{(\bar{V} + \sigma_V - \theta)}{\Delta V}\right]} \quad (15)$$

that is a sigmoid function with a very small width ΔV (we chose this parameter since it represents the natural scale of the absorbing barrier) to preserve the derivability and smoothness of the current-to-rate gain function. This is a key step to define an effective expression for smoothly merging the two approximations (VD and MC) when the regime transitions from fluctuation- to drift-driven.

Finally, we get the following current-to-rate gain function:

$$\mathcal{F}(v_e, v_i, s) = \frac{1}{\sigma^2} \int_{-\infty}^{\theta+5\Delta V} dV \int_{\max(V, V_r)}^{\theta+5\Delta V} du \times e^{-\frac{1}{\tau_m \sigma^2} \int_V^u [f(v) + f_1(v, \bar{g}_e, \bar{g}_i) - (1-s)(g_e + g_i)(v - \bar{V})/g_i] dv}. \quad (16)$$

This formulation is valid in absence of synaptic integration ($\tau_\alpha = 0$), but its firing-rate estimation is rather accurate even in presence of coloured input, as expected according to [26], as shown in Fig. 2.

To check the effectiveness of Eq. (16), we compared the \mathcal{F} obtained with the MC and the VD approximations, and with the state-dependent one, for varying excitatory and inhibitory input firing rates [Fig. 3(a)]. We report the respective errors [difference between theory and simulations, see Fig. 3(b)],

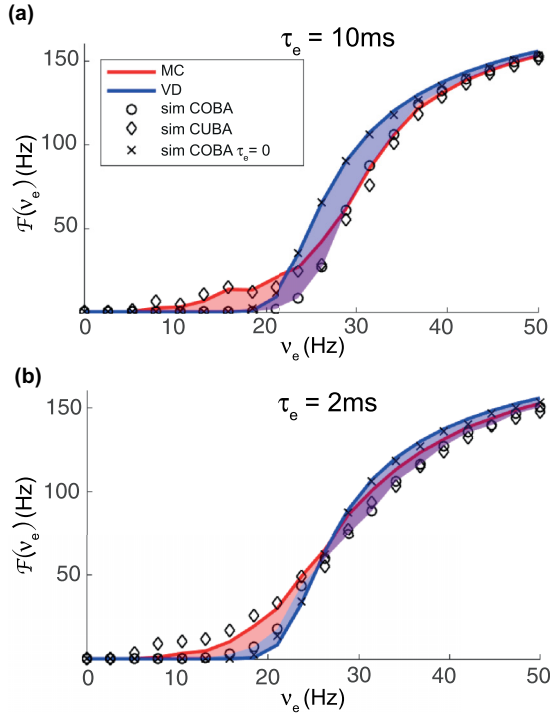


FIG. 2. Different scales of synaptic integration. Comparison between two different scales of synaptic integration 5 ms (a) and 1 ms (b). Circles and crosses are COBA simulations, respectively, with and without synaptic filter. The diamonds are CUBA simulations. MC and VD approximations in red (light gray) and blue (dark gray) fit almost exactly CUBA simulations with synaptic filter and COBA simulations without synaptic filter, respectively.

showing that in our approach they are smaller and distributed in a narrower region in the v_e, v_i plane.

We considered also the adaptation variable $W(t)$ with a relaxation timescale $\tau_w = 500$ ms, and compared the prediction with the simulations for the three models, observing an optimal estimation for the state-dependent one [Fig. 3(c)].

D. Application: Population dynamics

We applied our result for describing an effective mean-field dynamics for the canonically considered minimal structure of a cortical network, namely, two coupled population of neurons, one excitatory (regular spiking, RS) and one inhibitory (fast spiking, FS). RS neurons also have a spike frequency adaptation mechanism [see Fig. 4(a)]. The external input is provided by increasing the excitatory firing rate in the input of both the population by an amount of $v_{\text{ext}} = 6$ Hz. Neuronal parameters are specified in Table I. The probability of connection is $p = 0.25$.

We define the MF dynamics for the average excitatory and inhibitory firing rates of the network (respectively, v_e and v_i) following the approach used in Ref. [45]:

$$\begin{aligned} \tau_e \frac{dv_e}{dt} &= \mathcal{F}_e(v_e, v_i, W) - v_e + \sigma_e \xi_e(t) \\ \tau_i \frac{dv_i}{dt} &= \mathcal{F}_i(v_e, v_i) - v_i + \sigma_i \xi_i(t) \\ \frac{dW}{dt} &= -\frac{W}{\tau_w} + b v_e - a(\bar{V}_e - E_l) \end{aligned} \quad (17)$$

where we also considered the adaptation variable W . The parameter b and a are the same as in Eq. (1). τ_e and τ_i are the same as the membrane potential time scales. ξ_α are white normal noises, and σ_α are the extents of the noise. $\bar{V}_e = \langle V(t) \rangle_e$ is the population average membrane potential. This is evaluated by integrating its deterministic differential equation. The adaptation corresponds to an additional term in the first infinitesimal moment, so that we can define

$$\mu_w = \mu - \frac{W}{C}. \quad (18)$$

By changing the parameters, it is possible to set the network in different dynamical states. The asynchronous irregular (AI) is obtained by the parameters defined above. The slow oscillations (SO) are achieved by multiplying the probability of connection between excitatory neurons by a factor 1.15, increasing the excitatory adaptation strength to $b = 0.02$ nA and decreasing the external input to $v_{\text{ext}} = 0.95$ Hz.

The different regimes can be studied by the means of standard techniques used in dynamical systems theory, e.g., null-clines representation [see Fig. 4(b)]. Each null-cline represents the region where the derivative is zero for a certain variable (respectively, black line for v_e and orange dashed line for W), and the intersection between them is a fixed point that can be either stable or unstable. The green (light gray) line represents the dynamics in the plane (v_e, W) . This analysis is performed for the different choices of parameters and thus for the different dynamical conditions AI and SO. Figure 4(c) presents an example of the time-course of the dynamics for the two regimes in green (light gray) and red (dark gray), respectively, for v_e and v_i . We eventually reported the average firing-rate time course for a network of spiking neurons with the same choice of parameters as in the previous analysis [Fig. 4(d)], confirming that the predicted dynamics turns out to match the spiking simulations [same color coding as Fig. 4(c)].

E. Robustness of the prediction: Need of a state-dependent approach

We tested the robustness of the mean-field dynamical predictions by exploring for the network for different parameter values different the network parameters. First we changed the the external input to the network in the AI regime, observing the change in the stationary excitatory (green—light gray) and inhibitory (red—dark gray) firing rates of the network [Fig. 5(a)]. When only one of the two approximation is considered (top and middle panel) the mismatch between the theory (solid lines) and simulations (circles:mean, bars:standard deviation) is relevant, while the state-dependent approximation correctly reproduces the network behavior (bottom panel).

However, in the SO regime we modulated the adaptation b and analyzed the change in up and down states duration [Figs. 5(b) and 5(c)]. Again, the first two approximations taken alone poorly predict the dynamics observed in the spiking simulations (top and middle panels), while such task was performed quite well in the state-dependent approach (bottom panel).

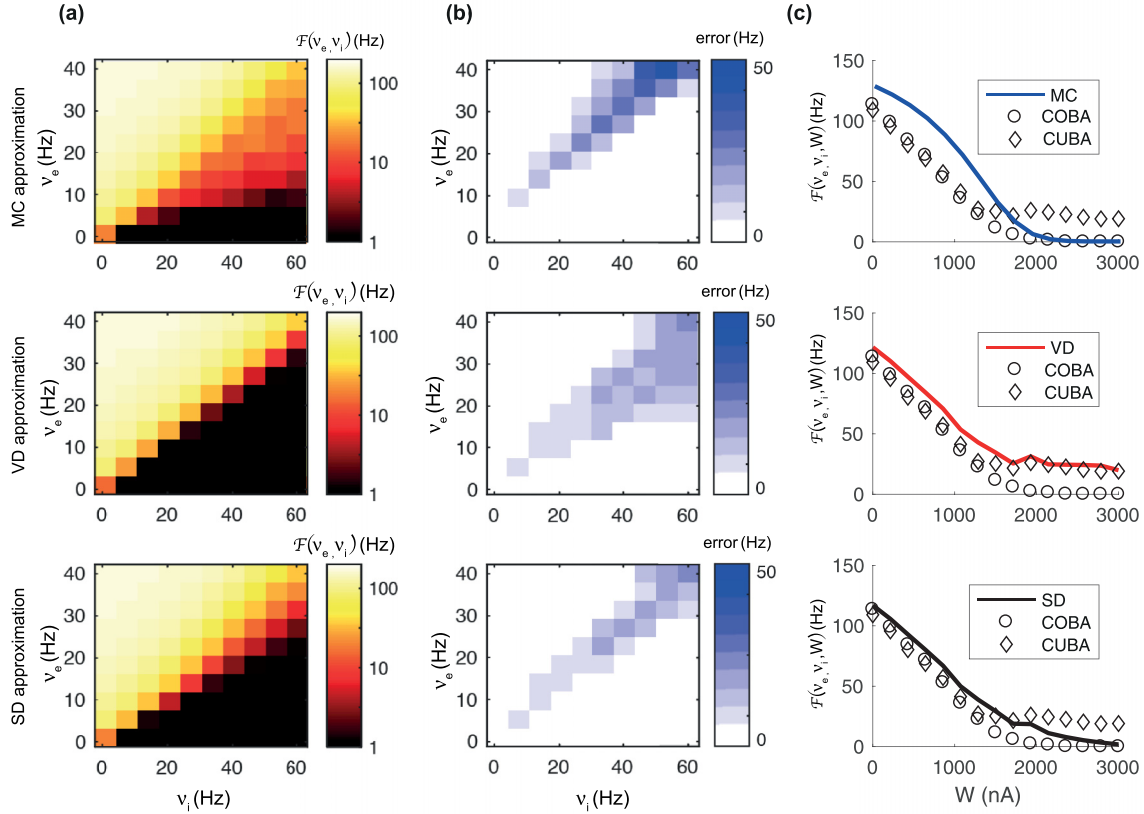


FIG. 3. State-dependent mean-field approximation. (a) Theoretical predicted firing rate (color-coded) for the MC, VD, and the state-dependent approximation. (b) Difference between the three theoretical models and the firing rate estimated in simulations. (c) Theoretical predicted firing rate (solid line) and firing rate from simulations for COBA and CUBA (respectively, circles and diamonds) for the three theoretical approximations.

F. Sublinear stimulus suppression

One of the main advantages of our approach is the possibility to compare the effect of COBA and CUBA synapses at the level of the population dynamics. We can indeed use the MC approximation for CUBA (the VD approximation is not necessary in this case) networks and the SD approximation for COBA network and perform a well defined comparison (see Fig. 2). To test the role of COBA synapses we consider a phenomenon recently observed in the visual cortex, and giving rise to a sublinear population response to external stimuli which plays a key role to decode correctly different stimuli [23]. To evaluate the capability of our theoretical description to capture such phenomenology, we study the nonlinearity of the network response to the presentation of two consecutive stepwise stimuli [$v_{\text{ext}}^{\text{stim}}(t) = v_1(t) + v_2(t)$, see Fig. 6(a)]. This is obtained by providing an additional input $v_{\text{ext}}^{\text{stim}}(t)$ to the external input v_{ext} provided to the network. We then compared the mean-field response to such stimulus for an excitatory-inhibitory network with COBA and CUBA input integration, respectively. In Fig. 6(a) the difference $\delta v_e(t) = v_e(t) - \bar{v}_e$ between the firing rate of the excitatory population with and without stimulation [$v_e(t)$ and \bar{v}_e , respectively] is shown.

We then compared the response predicted under the linear input-output hypothesis and the predictions from our approximated mean-field theory.

The linear response to the two stimuli $v_1(t)$ and $v_2(t)$ is assumed to be given by the sum of the responses to the two isolated stimuli [$\delta v_e^{\text{lin}} = \delta v_e^{(1)} + \delta v_e^{(2)}$]. As experimentally observed, we found that the system is sublinear (i.e., $\delta v_e - \delta v_e^{\text{lin}} < 0$) for both COBA and CUBA network [see Fig. 6(c)], although the intensity of the suppression is higher in the COBA model, as in Ref. [23]. This confirms the role of the COBA synapses in further emphasizing the differences in the response to two stimuli in sequence.

Due to the enhanced sensitivity of the COBA synapses to the working regime of membrane potential of the neurons, we expect the differences highlighted in Fig. 6 to be state-dependent. To investigate this aspect of the sublinear summation effect we measured $\delta v_e - \delta v_e^{\text{lin}}$ for different levels of the network activity, here modulated by changing the external input v_{ext} before the arrival of the two stimuli [see Fig. 7(a)].

As a result, we found that the suppression of the responses to the second stimulus is always stronger in COBA networks than those measured in networks with CUBA currents.

Intriguingly, such effect is even more apparent when v_{ext} is low.

The suppression enhancement is related to the change in the membrane potential after the first impinging stimulus. Indeed, the population average membrane potential in the COBA network appears to be more depolarized at the onset

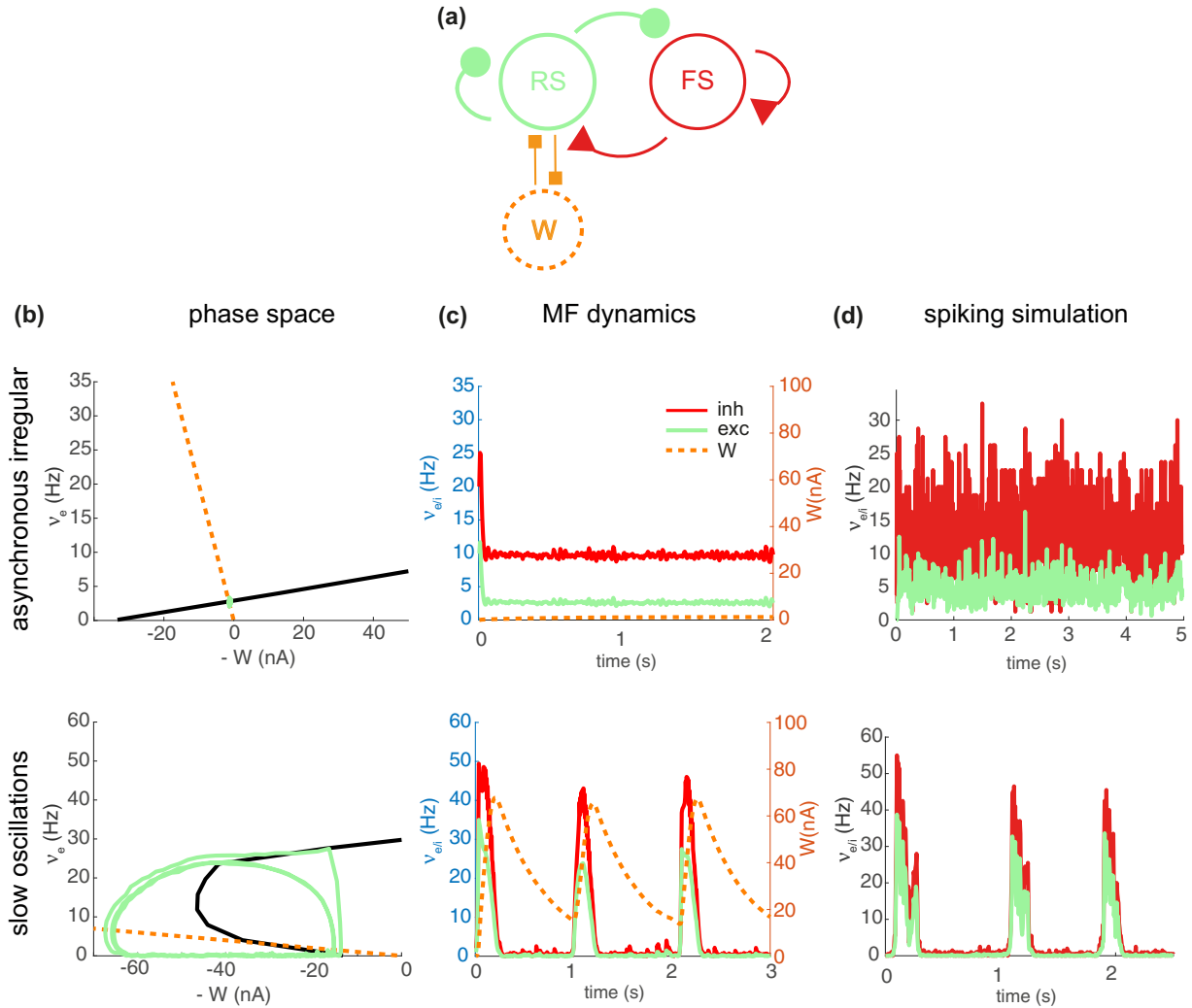


FIG. 4. Mean-field dynamics in a RS-FS network: (a) Sketch of the network structure. (b) Nullclines representation of the dynamical system in the phase space for two different dynamical regimes (top: asynchronous irregular; bottom: slow oscillations). Blue solid (dark gray solid) and orange dashed (light gray dashed) lines: Nullclines for the excitatory firing rate and the adaptation variables. The green (light-gray solid line) line represents the trajectory of the dynamics of excitatory firing rate in the phase-space. (c) Example of mean-field dynamics for the two different regimes, green (light gray) and red (dark gray) represent excitatory and inhibitory firing rates, respectively. (d) Average firing-rate dynamics of the spiking simulation. Green (light gray) and red (dark gray) represent excitatory and inhibitory firing rates, respectively.

time of the second stimulus (t_2) than at the beginning of the first stimulation (t_1) [Fig. 7(b)].

To the purpose of this comparison, the excitatory synaptic efficacy in CUBA networks is set to be proportional to $(E_e - V^*)$ where V^* is the average membrane potential in t_1 and represented by the dark blue line in Fig. 7(b).

Finally, we evaluate the current contribution during the second stimulation [$I_2^{stim} = g_e (E_e - V)$] for both COBA and CUBA networks [Fig. 7(c)]. In CUBA networks this contribution is almost unaffected by the changes of the membrane potential (dark blue line) while for COBA networks the current is reduced by the increase of V (light pink line), accounting for the stronger suppression observed in COBA networks.

III. DISCUSSION

The mean-field description of a large network of excitatory and inhibitory spiking neurons has been tackled analytically

on relatively simple models but often far from biophysical reality [19,20]. However, anatomically sophisticated models [8,16–18] are computationally consuming and very hard to be explored by mean of theoretical frameworks.

In the present paper, we proposed a tradeoff between these two possibilities. First we chose a neuron model which has an intermediate mathematical complexity but also a high physiological validity: the exponential integrate-and-fire neuron with spike frequency adaptation. Second, we consider voltage-dependent synapses (COBA) that so far made this problem difficult to be exactly solved.

To overcome the mathematical difficulty of solving a Fokker-Planck equation with a voltage-dependent noise, describing a conductance-based input, we proposed a mapping on a CUBA model, which has a known solution [19]. However, we showed that this mapping has to be state-dependent, since different approximations have to be considered in different regimes. Indeed, in the fluctuation-driven regime it

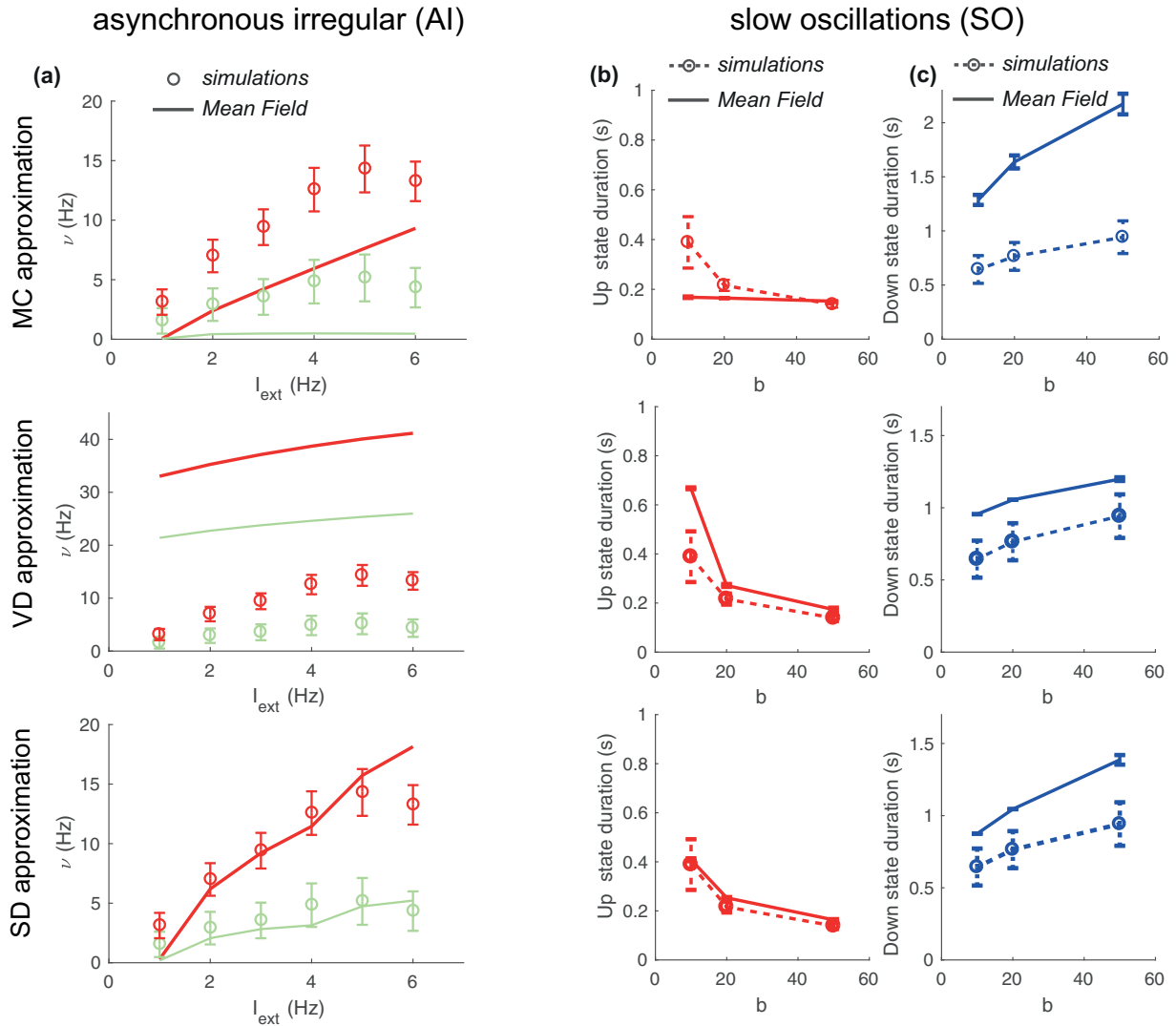


FIG. 5. State-dependent approximation is required to correctly capture the dynamics. (a) Predicted stationary excitatory and inhibitory firing rates—green (light gray) and red (dark gray) lines—as a function of the amount of external noise, compared with spiking simulations (circles). (b, c) Predicted up and down states durations (solid line) as a function of the adaptation strength b compared with spiking simulations (dashed line).

is possible to use a standard approximation that basically maps the COBA on a CUBA with rescaled membrane time scale [30].

Nevertheless, in the drift-driven regime this approximation is no longer providing a good description, and it has been shown only to work in a relatively simple model with instantaneous synapses and leaky integrate and fire neuron. Our analysis reported that this is no longer valid when a synaptic integration is considered since this that creates a strong interaction between conductances and membrane potential. Nevertheless, a different suitable approximation can be performed neglecting the fluctuations of the membrane potential, obtaining again an effective CUBA model where the variable the membrane potential V is frozen and replaced by a stochastic process with the same statistical moments. An analytic merge of the two approaches provides a good prediction of the firing rate in the whole phase space.

Making approximations is a natural way to simplify a problem and understand more easily the underlying mechanisms.

Our approach, since it relies on two different approximations, points out that the relevant aspects producing the observed dynamics are state-dependent. It allows to understand in which condition a single approximation works and when it doesn't, improving an intuitive understanding of the system.

Since neurons in cortical populations notoriously go across both noise and drift dominated regimes [46–48], to define a population mean-field dynamics requires to take into account a unified framework like the one we propose. To support this statement we have shown that when a single approximations have been considered the quality of predictions was extremely poor.

A unique transfer function reliable in various dynamical conditions is particularly relevant also because different population may be in different regimes or the same population can change regime across time, as in the case of slow oscillations.

We showed that our method is robust and flexible and successfully describes different population dynamical regimes, such as asynchronous irregular state and slow oscillations.

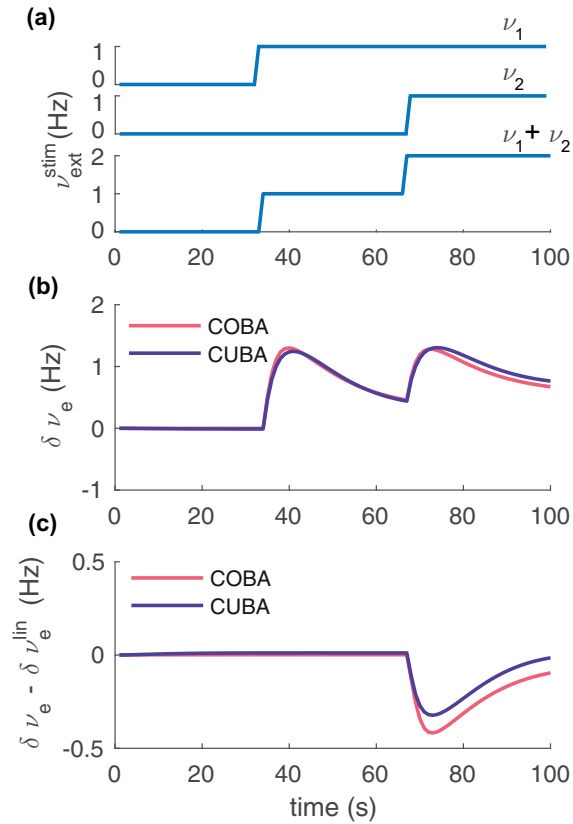


FIG. 6. Suppression of stimuli summation. (a) Input stimulus. (b) Response $\delta\nu_e$ to input stimuli for a COBA and a CUBA network of neurons, pink (light gray) and blue (dark gray), respectively. (c) Response to the input stimuli minus the linear prediction ($\delta\nu_e - \delta\nu_e^{\text{lin}}$), showing a stronger non linear suppression in the COBA network.

Our approach suggests a general method to perform a state-dependent mapping of neurons with COBA input on to CUBA input even with different types of neuron such as QIF and LIF.

Our model could be interpreted as an attempt to do a step forward to the development of analytic but still rich and realistic theories that allow to describe experimentally observed phenomenons [22].

Note that we did not investigate the fast-responses of the network as described by other theoretical efforts [49]. Considering only first-order ODE implies a limitation in describing very high-frequencies, however we focused on the out-of-equilibrium dynamics induced by spike-frequency adaptation, thus a dynamics unfolding on relatively long time scales. To include a delayed and filtered version of the firing rate (such as the one due to synaptic filtering) to induce resonant frequencies (in the gamma range, for instance) will be the subject of future studies.

We propose that the model can be naturally extended to more complicated structures, such as the thalamocortical loop and network with spatial extension. This would permit to test our model on experimental data recording the activity of populations of neurons over space where it may provide a mechanistic understanding of the emerging dynamics based on neurons voltage-based interactions.

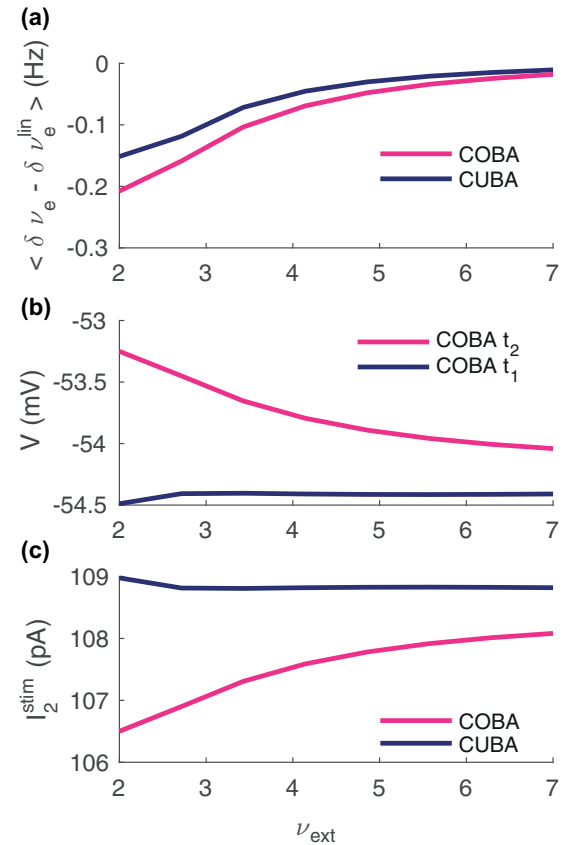


FIG. 7. Suppression of stimuli summation: parameter exploration. (a) Average summation suppression for different values of ν_{ext} (the external current before stimulation onset) for COBA and CUBA networks. (b) Average membrane potential of COBA networks before the first ($t = t_1$) and the second stimuli ($t = t_2$). (c) Synaptic current during the second stimulation in COBA and CUBA networks in pink (light gray) and blue (dark gray), respectively.

A semianalytic approach was proposed recently [34,36] which relies on a fitting of the transfer function to numerical simulations. This approach yields mean-field models of COBA neurons with good quantitative predictions. The main advantage provided by this “orthogonal” approach is to be potentially applicable to any neuronal model and to experimental data. On the other side, as being a semianalytic fit, it does not permit the same understanding of the dynamical mechanisms underlying the neurons response function as a principled approach like it does the one here proposed. More detailed comparison of the two approaches is the object of future directions and the knowledge derived from these two different approaches will help to make important steps forward towards an unified theory of mean-field models of COBA neurons.

ACKNOWLEDGMENTS

This project has received funding from the CNRS and the European Union’s Horizon 2020 Framework Programme for Research supported by the CNRS and the European Union (Human Brain Project, H2020-720270 and H2020-785907).

- [1] A. Maccione, M. Gandolfo, S. Zordan, H. Amin, S. D. Marco, T. Nieuws, G. N. Angotzi, and L. Berdondini, *Brain Res. Bull.* **119**, 118 (2015).
- [2] C. Capone, G. Gigante, and P. Del Giudice, *Sci. Rep.* **8**, 17056 (2018).
- [3] I. M. Park, M. L. Meister, A. C. Huk, and J. W. Pillow, *Nat. Neurosci.* **17**, 1395 (2014).
- [4] W. Truccolo, L. R. Hochberg, and J. P. Donoghue, *Nat. Neurosci.* **13**, 105 (2010).
- [5] J. W. Pillow, J. Shlens, L. Paninski, A. Sher, A. M. Litke, E. Chichilnisky, and E. P. Simoncelli, *Nature* **454**, 995 (2008).
- [6] E. M. Izhikevich, *IEEE Trans. Neural Netw.* **14**, 1569 (2003).
- [7] R. Brette and W. Gerstner, *J. Neurophysiol.* **94**, 3637 (2005).
- [8] H. Markram, *Nat. Rev. Neurosci.* **7**, 153 (2006).
- [9] C. Capone, E. Pastorelli, B. Golosio, and P. S. Paolucci, *Sci. Rep.* **9**, 8990 (2019).
- [10] C. Capone, B. Rebollo, A. Muñoz, X. Illa, P. Del Giudice, M. V. Sanchez-Vives, and M. Mattia, *Cereb. Cortex* **29**, 319 (2019).
- [11] C. Capone and M. Mattia, *Sci. Rep.* **7**, 39611 (2017).
- [12] M. Lundqvist, A. Compte, and A. Lansner, *PLoS Comput. Biol.* **6**, e1000803 (2010).
- [13] N. Brunel, *Neural Comput.* **11**, 1621 (1999).
- [14] M. Mattia and P. Del Giudice, *Phys. Rev. E* **66**, 051917 (2002).
- [15] A. Treves, *Network: Comput. Neural Syst.* **4**, 259 (1993).
- [16] R. D. Traub, R. Miles, and R. K. Wong, *IEEE Eng. Med. Biol. Mag.* **7**, 31 (1988).
- [17] R. D. Traub, D. Contreras, M. O. Cunningham, H. Murray, F. E. LeBeau, A. Roopun, A. Bibbig, W. B. Wilent, M. J. Higley, and M. A. Whittington, *J. Neurophysiol.* **93**, 2194 (2005).
- [18] E. M. Izhikevich and G. M. Edelman, *Proc. Natl. Acad. Sci. U.S.A.* **105**, 3593 (2008).
- [19] N. Brunel, *J. Comput. Neurosci.* **8**, 183 (2000).
- [20] N. Brunel and P. E. Latham, *Neural Comput.* **15**, 2281 (2003).
- [21] N. Fourcaud-Trocmé, D. Hansel, C. Van Vreeswijk, and N. Brunel, *J. Neurosci.* **23**, 11628 (2003).
- [22] W. Paulus and J. C. Rothwell, *J. Physiol.* **594**, 2719 (2016).
- [23] S. Chemla, A. Reynaud, M. di Volo, Y. Zerlaut, L. Perrinet, A. Destexhe, and F. Chavane, *J. Neurosci.* **39**, 4282 (2019).
- [24] H. C. Tuckwell, *Introduction to Theoretical Neurobiology, Vol. 2: Nonlinear and Stochastic Theories* (Cambridge University Press, Cambridge, 1988).
- [25] G. Gigante, M. Mattia, and P. Del Giudice, *Phys. Rev. Lett.* **98**, 148101 (2007).
- [26] N. Brunel and S. Sergi, *J. Theor. Biol.* **195**, 87 (1998).
- [27] R. Moreno-Bote and N. Parga, *Phys. Rev. Lett.* **92**, 028102 (2004).
- [28] P. I. M. Johannesma, in *Neural Networks*, edited by E. R. Caianiello (Springer, Berlin/Heidelberg, 1968), pp. 116–144.
- [29] A. N. Burkitt, *Biol. Cybern.* **85**, 247 (2001).
- [30] M. J. E. Richardson, *Phys. Rev. E* **69**, 051918 (2004).
- [31] F. Apfaltrer, C. Ly, and D. Tranchina, *Network* **17**, 373 (2006).
- [32] M. Augustin, J. Ladenbauer, and K. Obermayer, *Front. Comput. Neurosci.* **7**, 9 (2013).
- [33] W. Nicola, C. Ly, and S. A. Campbell, *SIAM J. Appl. Math.* **75**, 2333 (2015).
- [34] Y. Zerlaut, S. Chemla, F. Chavane, and A. Destexhe, *J. Comput. Neurosci.* **44**, 45 (2018).
- [35] M. Carlu, O. Chehab, L. Dalla Porta, D. Depannemaecker, C. Héricé, M. Jedynek, E. Köksal Ersöz, P. Muratore, S. Souihel, C. Capone, Y. Zerlaut, and M. di Volo, *J. Neurophysiol.* (to be published).
- [36] M. di Volo, A. Romagnoni, C. Capone, and A. Destexhe, *Neural Comput.* **31**, 653 (2019).
- [37] M. Okun and I. Lampl, *Nat. Neurosci.* **11**, 535 (2008).
- [38] M. Avermann, C. Tomm, C. Mateo, W. Gerstner, and C. C. Petersen, *J. Neurophysiol.* **107**, 3116 (2012).
- [39] M. V. Sanchez-Vives, M. Massimini, and M. Mattia, *Neuron* **94**, 993 (2017).
- [40] A. N. Burkitt, *Biol. Cybern.* **95**, 1 (2006).
- [41] N. Brunel and X.-J. Wang, *J. Neurophysiol.* **90**, 415 (2003).
- [42] N. Brunel and X.-J. Wang, *J. Comput. Neurosci.* **11**, 63 (2001).
- [43] D. J. Amit and M. Tsodyks, *Network: Comput. Neural Syst.* **2**, 259 (1991).
- [44] D. J. Amit and N. Brunel, *Cerebral Cortex* **7**, 237 (1997).
- [45] S. El Boustani and A. Destexhe, *Neural Comput.* **21**, 46 (2009).
- [46] E. J. Ramcharan, J. W. Gnadt, and S. M. Sherman, *Visual Neurosci.* **17**, 55 (2000).
- [47] M. V. Sanchez-Vives and D. A. McCormick, *Nat. Neurosci.* **3**, 1027 (2000).
- [48] A. Destexhe and D. Contreras, *Sleep and Anesthesia* (Springer, Berlin, 2011), pp. 69–105.
- [49] E. Ledoux and N. Brunel, *Front. Comput. Neurosci.* **5**, 25 (2011).